Journal of Structural Chemistry, Vol. 54, Supplement 1, pp. S130-S136, 2013

^{11}B NMR STUDY OF $Ho_{1-x}Y_xAl_3(BO_3)_4$ MULTIFERROICS

© **Yu. N. Ivanov, A. A. Sukhovskii, and N. V. Volkov**

UDC 548.7

The ^{11}B NMR method is used to study the crystals of trigonal alumina borates $Ho_{1-x}Y_xAl_3(BO_3)_4$ (x = 0, 0.5, 1). The temperature-field evolution of quadrupole and hyperfine interactions in these compounds is studied and described.

DOI: 10.1134/S0022476613070135

Keywords: NMR, multiferroics, quadrupole interaction, hyperfine interaction.

INTRODUCTION

The interest of researchers to noncentrosymmetric $RAl_3(BO_3)_4$ crystals has increased recently [1]. It may be explained by strong magnetoelectric effects of some crystals of this family [2]. These properties are promising in terms of practical application in modern electronics as well as the fundamental research in solid state physics for the study of interactions in the magnetic and electric subsystems of crystals. The nuclear magnetic resonance (NMR) of quadrupole nuclei is sensitive to fluctuations in the local electric and magnetic fields in the locations of the nuclei; thus, it may be applied to determine the micromechanisms of multiferroic properties in these compounds.

This work shows the ^{11}B NMR spectra of trigonal $Ho_{1-x}Y_xAl_3(BO_3)_4$ single crystals (x = 0, 0.5, 1) and analyzes the NMR advantages for the study of the temperature-field evolution of local interactions, including those caused by changes in the electronic state of the rare-earth ion.

EXPERIMENTAL

Single crystals $RAl_3(BO_3)_4$ (R = Ho, Y, $Ho_{1/2}Y_{1/2}$) were grown from the solution-melt based on bismuth trimolybdate and lithium molybdate [3] using the method described in [4]. The crystals of this family are isomorphic to $CaMg_3(CO_3)_4$ huntite at room temperature and have a trigonal system and the space group $R32$ [5]. The structure is based on the helical chains of AlO_6 octahedra joined by common edges and elongated along the c axis. Each rare-earth ion is coordinated by six oxygen ions forming triangular RO_6 prisms. These prisms are separated by BO_3 triangles and do not share oxygen atoms. Both BO_3 triangles and RO_6 prisms link three chains of AlO_6 octahedra.

There are two structurally non-equivalent positions of boron in the structure, i.e. B1 and B2, with B1 being located in a special position on the threefold axis, and B2 in the general position. Both B1 and B2 ions lie in the plane of oxygen triangles (Fig. 1), but the corresponding $(B2)O_3$ triangle is distorted.

It is significant for this study that two adjacent rare-earth ions are located at the same distance of 3.622 Å from the B1 atom (towards the c axis). For the B2 ion the corresponding distances are 2.989 Å; however, unlike B1, in this case three

L. V. Kirensky Institute of Physics, Siberian Division, Russian Academy of Sciences, Krasnoyarsk; yuni@iph.krasn.ru. Translated from *Zhurnal Strukturnoi Khimii*, Vol. 54, Supplement 1, pp. S132-S138, 2013. Original article submitted January 25, 2013.

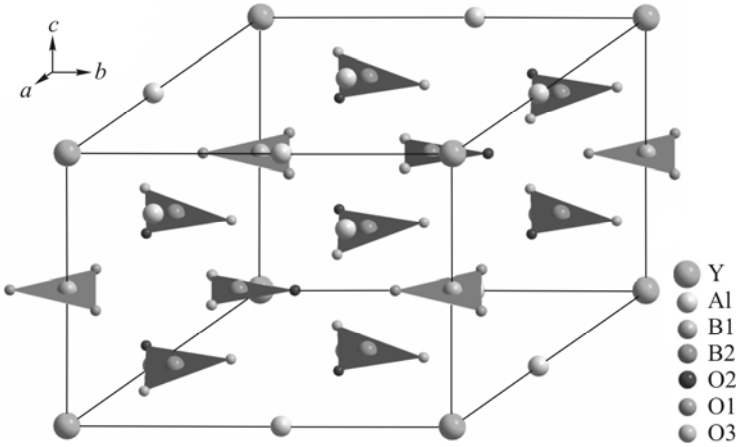

Fig. 1. The structure of $YAl_3(BO_3)_4$.

atoms do not lie on the straight line (R–B2–R angle is ~160°). The distances to the rare-earth ions that are next to the nearest ones are considerably larger.

The ^{11}B NMR spectra were recorded on an AVANCE-300 NMR pulse spectrometer (^{11}B Larmor frequency F = 96.3 MHz) and a home-made continuous-wave NMR spectrometer with the ^{11}B Larmor frequency within the range 12-17 MHz. Note that when noncentrosymmetric crystals with high piezoelectric properties are studied by pulse NMR, some specific difficulties occur, which are related to the electro-acoustic ringing of the samples. The latter masks the NMR signal so often that it is impossible to record the spectra. There is a number of methods that provide the suppression of this effect: electrostatic shields, damping of the sample, and special pulse programs. However, the use of all these methods ensured the recording of the ^{11}B NMR pulse spectra only in the $YAl_3(BO_3)_4$ crystal. Therefore, the major part of the work was performed on the continuous-wave NMR spectrometer.

RESULTS AND DISCUSSION

The ^{11}B nuclei have spin $I = 3/2$ and, thus, the electric quadrupole moment. The resonance in the nuclei with the quadrupole moment informs about the gradient magnitude and symmetry of the intracrystalline electric fields in the nucleus location.

In the presence of a strong external magnetic field H_0 with the energy of the Zeeman interaction significantly exceeding the energy of the interaction between the nucleus quadrupole moment and the intercrystalline field, the latter causes the excitation of equidistant Zeeman levels and the NMR line splitting into $2I$ components symmetrical to the Larmor precession frequency in the field. Hence, the ^{11}B NMR spectra consist of triplets with the intensity ratio of 2:3:2, the number of which for the single crystal is generally determined by the number of magnetically nonequivalent ^{11}B nuclei. The quadrupole splitting values depend on the crystal orientation in the magnetic field, and the position of the lines is determined by the relation [6]

$$\omega_{m\leftrightarrow m-1} = \omega_0 + \frac{3e^2qQ(2m-1)}{8I(2I-1)\hbar}(3\cos^2\theta - 1 + \eta\sin^2\theta\cos 2\phi), \quad (1)$$

where ω_0 is the Larmor frequency; θ is the angle between H_0 and the main z axis of the electric field gradient tensor (EFG); ϕ is the angle between the main x axis of the EFG tensor and the intersection point of the plane perpendicular to H_0 and plane perpendicular to the main z axis of the EFG tensor; η is the asymmetry parameter of the EFG tensor.

Fig. 2 shows the orientation dependence of quadrupole splittings when $YAl_3(BO_3)_4$ crystal is rotated around the b axis. Following the dependence in Fig. 2 and considering the crystal symmetry, the EFG tensor parameters can be completely determined for two structurally nonequivalent positions of boron atoms: B1 and B2 (Table 1).

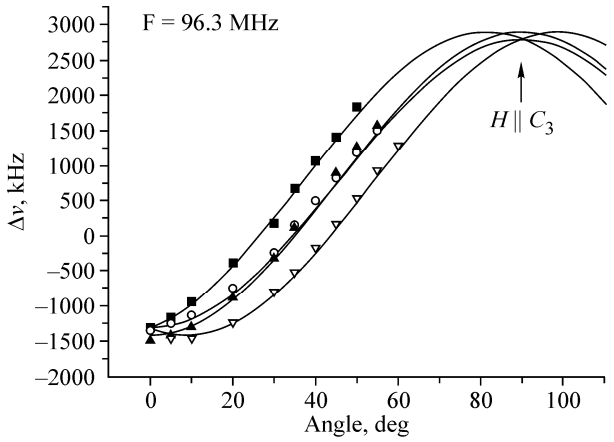

Fig. 2. Orientation dependence of quadrupole splittings when the $YAl_3(BO_3)_4$ crystal is rotated around the *b* axis.

TABLE 1. EFG Tensor Parameters for Two Structurally Nonequivalent Positions of Boron Atoms in $YAl_3(BO_3)_4$

B1				B2			
Main values of EFG tensors Φ_{ii} (kHz)	Direction cosines (with respect to orthogonal axes)			Main values of EFG tensors Φ_{ii} (kHz)	Direction cosines (with respect to orthogonal axes)		
	X	*Y*	*Z* (*c*3)		*X*	*Y*	*Z* (*c*3)
–1445	1	0	0	–1376	0.9848	0	0.1733
–1445	0	1	0	–1547	0	1	0
2890	0	0	1	2923	–0.1733	0	0.9848

As can be seen from Table 1, there are two types of EFG tensors: axially symmetric and triaxial ones. The former is attributed to boron atoms located on the threefold axis (3*b* position), while the latter to boron atoms in the general position (9*e* position). This is fully consistent with the structure of the $YAl_3(BO_3)_4$ crystal [5].

There are no points in some parts of the dependence due to large quadrupole splitting values (several MHz), which poses experimental difficulties. However, the EFG tensor parameters can also be found from the orientation dependence of the second-order quadrupole shifts of the central component. These shifts are determined by the following relation [7]:

$$\omega_{1/2\leftrightarrow -1/2} = \omega_0 - \frac{\omega_Q^2 (I(I+1) - 3/4)}{6\omega_0} (A(\phi)\cos^4\theta + B(\phi)\cos^2\theta + C(\phi)), \quad (2)$$

where

$$A(\phi) = -\frac{27}{8} + \frac{9}{4}\eta\cos 2\phi - \frac{3}{8}\eta^2\cos^2 2\phi;$$

$$B(\phi) = \frac{30}{8} - 2\eta\cos 2\phi - \frac{1}{2}\eta^2 + \frac{3}{4}\eta^2\cos^2 2\phi;$$

$$C(\phi) = -\frac{3}{8} + \frac{1}{3}\eta^2 - \frac{1}{4}\eta\cos 2\phi - \frac{3}{8}\eta^2\cos^2 2\phi;$$

$$\omega_Q = \frac{3e^2qQ}{2I(2I-1)\hbar}.$$

Following relation 2, the magnitude of the shifts is inverse to the Larmor frequency. As was ascertained, in the field of ~1 T these shifts significantly exceed the ^{11}B NMR line width, and the EFG tensors can be found with high accuracy. Hence, a lower frequency and the measurement of the second-order shifts solve the problem of too large quadrupole splittings, while the use of the continuous-wave recording method solves the above problem of acoustic ringing. Fig. 3 (solid lines) shows the

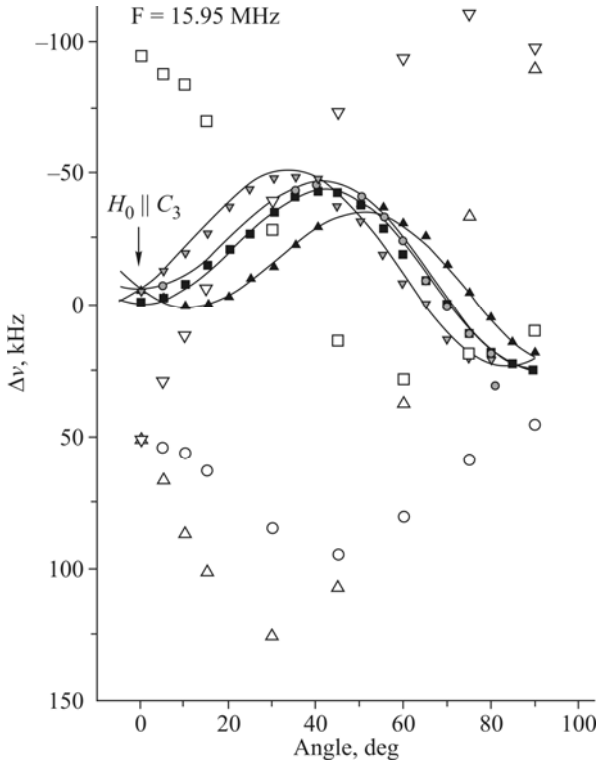

Fig. 3. Orientation dependences of the second-order ^{11}B shifts in $YAl_3(BO_3)_4$ (solid lines) and $HoAl_3(BO_3)_4$.

orientation dependence of the second-order quadrupole shifts of the central component in the $YAl_3(BO_3)_4$ crystal. The EFG tensors obtained from it using relation (2) correspond to Table 1 data.

As stated above, the NMR spectra of the $HoAl_3(BO_3)_4$ crystal were recorded only using the continuous-wave method. Fig. 3 shows the orientation dependence of the second-order quadrupole shifts of the central component in the $HoAl_3(BO_3)_4$ crystal measured under the same conditions as the dependence for $YAl_3(BO_3)_4$. The difference in the orientation dependences of the NMR spectra of two isostructural crystals is likely to be attributed to the presence of paramagnetic ions in the $HoAl_3(BO_3)_4$ crystal. The magnetic moments of the paramagnetic ions create magnetic fields on both their own nuclei and the nuclei of other ions, and their constant component is called the local field. For the nuclei of diamagnetic ions the main part of the local field is determined by the hyperfine interactions, i.e. decompensation of their own electron shells induced by paramagnetic ions. The main reasons for this decompensation are the overlap of the electronic shells of para- and diamagnetic ions and the chemical bond covalence. When *S* shells are decompensated, the magnitude of the hyperfine field on the diamagnetic nucleus is determined by the so-called Fermi contact interaction. This part of the hyperfine field does not depend on the crystal orientation in the external magnetic field; therefore, it cannot account for the difference in the orientation dependences of the NMR spectra of $HoAl_3(BO_3)$ and $YAl_3(BO_3)$ crystals. In the case of the decompensation of a shell with a non-zero orbital quantum number, the magnitude of the hyperfine field depends on the orientation of these orbitals relative to the direction of the external magnetic field. If the electron density is distributed symmetrically to the line linking the para- and diamagnetic ions, then the hyperfine magnetic field value depends on the angle γ between the external magnetic field and the symmetry axis of the electron density distribution according to the following law:

$$H_{\text{loc}}^{(p)} = \frac{1}{g\mu_0}\sum_i (A_{\sigma i} - A_{\pi i})(1-\cos^2\gamma)\overline{S}_{zi}, \quad \overline{S}_z = \frac{CH_0}{T}, \tag{3}$$

where *g* is the nuclear *g* factor, μ_0 is the nuclear magneton, *C* is the constant, $\overline{S}_{zi}$ is the average value of the spin projection to H_0, A_σ, A_π are the parameters of the anisotropic indirect hyperfine interaction.

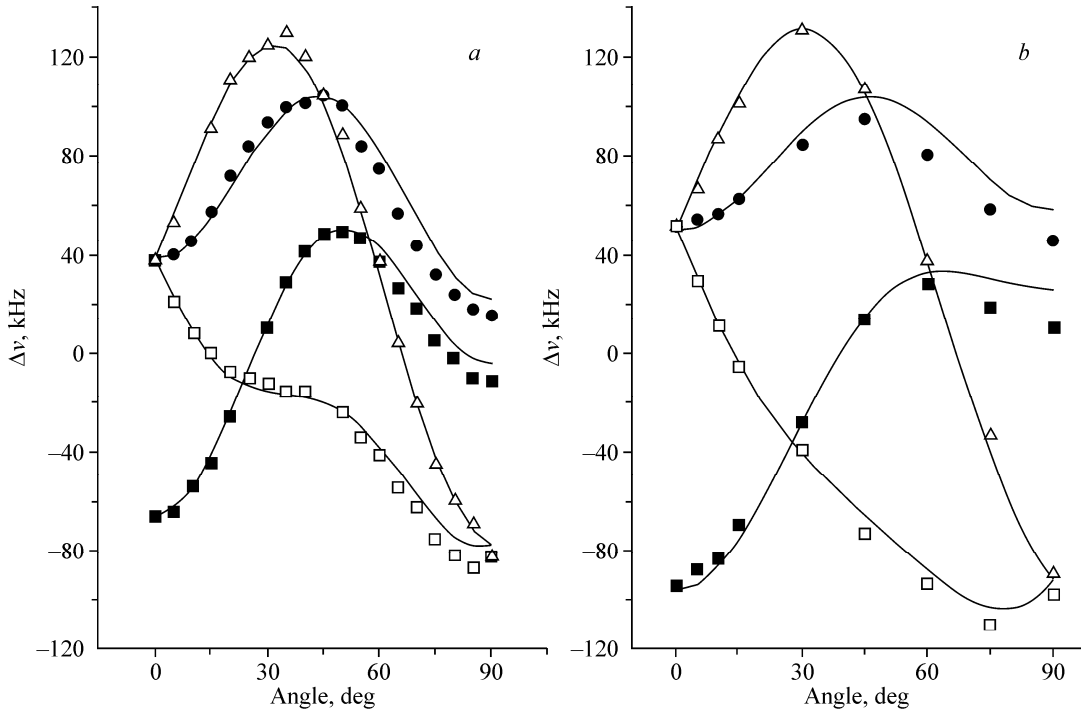

Fig. 4. Orientation dependences of the ^{11}B NMR spectra in the $HoAl_3(BO_3)$ crystal in the magnetic fields of 0.87 T (*a*) and 1.31 T (*b*).

Assuming that only the adjacent holmium atoms contribute to the local field on boron atoms, from the structural data [8] one can calculate the dependences of the angles γ_i for all structural positions of boron atoms from the direction of the external magnetic field; while from the orientation dependences of the ^{11}B NMR spectra one can obtain the EFG tensor parameters on boron atoms as well as the hyperfine interaction parameters. As in the $YAl_3(BO_3)$ crystal, in $HoAl_3(BO_3)$ there are two types of EFG tensors on boron atoms, and their parameters correlate well with Table 1 data. Following relations (2) and (3), with an increase in the external magnetic field the local fields increase proportionally, while the second-order quadrupole shifts decrease inversely to the field. This makes it possible to independently verify the accuracy of the assumption and measurements of the parameters. Fig. 4 shows the experimental orientation dependences of the ^{11}B NMR spectra in the $HoAl_3(BO_3)$ crystal (dots) in the magnetic fields of 0.87 T and 1.31 T respectively. The orientation dependences (solid lines) calculated from the obtained parameters correlate well with the respective experimental values.

One of the controversial questions of the structure of the $Ho_{1/2}Y_{1/2}Al_3(BO_3)$ mixed crystal is the distribution of yttrium and holmium atoms in the crystal. This problem is unlikely to be solved by the traditional diffraction methods. However, the ^{11}B NMR spectra of the mixed crystal depend on the distribution features, which helps obtain the necessary data. As stated above, the EFG tensor parameters on boron atoms undergo only minor changes when the adjacent holmium ions are substituted for yttrium, since the charge distribution in the crystal remains unchanged (therefore, the EFG tensors on the corresponding boron nuclei in $YAl_3(BO_3)$ and $HoAl_3(BO_3)$ crystals coincide). However, the local fields change drastically when the paramagnetic holmium ion is substituted for the diamagnetic yttrium one. There are two rare-earth ions in the immediate vicinity of each boron atom. If both ions are diamagnetic yttrium, then the local field on the corresponding boron atom is zero, and the position of ^{11}B NMR spectral lines is determined only by the quadrupole interaction. If both ions are paramagnetic holmium, then the local field coincides with the corresponding field in the $HoAl_3(BO_3)$ crystal. If the ions are different, in order to calculate the local field the summation in relation (3) should be performed only for holmium ions. Thus, the positions of ^{11}B NMR spectral lines can be obtained for all possible configurations of the immediate vicinity of four magnetically nonequivalent boron atoms (Fig. 5). Altogether, there should be 15 lines in the ^{11}B NMR spectrum in the general orientation of the $Ho_{1/2}Y_{1/2}Al_3(BO_3)$ crystal: 3 lines from the boron atom in the specific position and 12 lines from

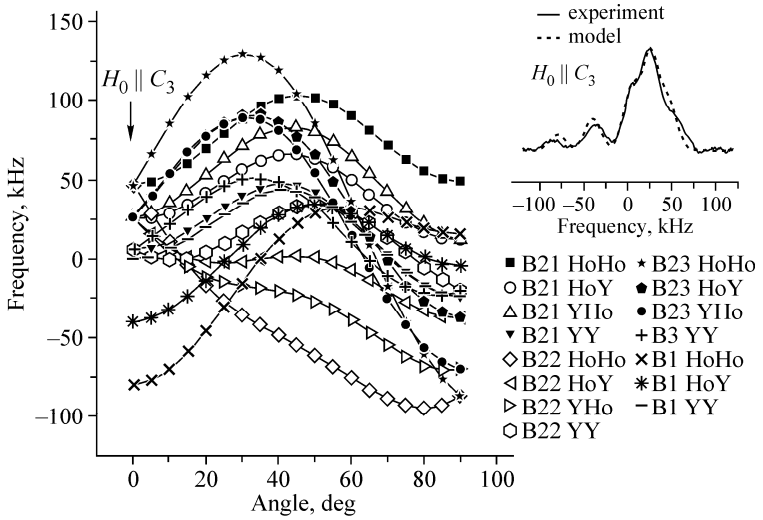

Fig. 5. Position of central lines of the ^{11}B NMR spectra in the $HoAl_3(BO_3)$ crystal when rotated around the *b* axis. The inset shows the experimental and calculated ^{11}B NMR spectra in the magnetic field orientation along the C_3 axis.

boron atoms in the general position. The intensity of each line is proportional to the number of boron atoms with the corresponding environment. Even in the specific orientation of the magnetic field along the C_3 axis of the crystal there are 6 spectral lines, and it is impossible to determine either the position or intensity of separate lines. In order to obtain the information on the intensity of spectral components we synthesized the NMR spectrum using the calculated positions of components and the same width as in the ^{11}B NMR spectra in the $HoAl_3(BO_3)$ crystal. The best correlation of the synthesized spectra with the experimental ones for all crystal orientations in the magnetic field was observed for the equiprobable distribution of yttrium and holmium ions in the corresponding positions. To illustrate it, Fig. 5 (inset) shows a comparison of the experimental and calculated ^{11}B NMR spectra in the orientation of the magnetic field along the C_3 axis in the $Ho_{1/2}Y_{1/2}Al_3(BO_3)$ crystal.

The study of the temperature dependences of the ^{11}B NMR spectra in the $YAl_3(BO_3)$ crystal has shown that within the temperature range of 300-100 K the position of the lines does not alter. Hence, the EFG tensor parameters on boron nuclei remain unchanged, which indicates that atoms in the $YAl_3(BO_3)$ crystal lattice do not shift within this temperature range. In the $HoAl_3(BO_3)$ crystal the splitting of the NMR spectral lines of boron tends to increase with a decrease in the temperature. In order to determine the type of the interaction, i.e. quadrupole or hyperfine, under which these changes occur, we measured the temperature dependences of the ^{11}B NMR spectra with the magnetic field orientation at 70° to the C_3 axis. In this orientation the lines of structurally and magnetically nonequivalent positions of boron are well resolved; and for one atom (B22) the position of the lines is entirely determined only by the hyperfine interaction, while for another one (B23) it is almost completely determined by the quadrupole interaction. According to the analysis of all ^{11}B NMR lines in the $HoAl_3(BO_3)$ crystal, it was ascertained that in the temperature range of 300-100 K only indirect hyperfine interaction alters, with this change being due to the increase in $\overline{S}_{zi}$ with a decrease in the temperature.

CONCLUSIONS

In conclusion, we would like to note that in $Ho_{1-x}Y_xAl_3(BO_3)_4$ compounds (x = 0, 0.5, 1) the EFG tensors on boron nuclei in the corresponding positions coincide. The parameters of these tensors do not alter within experimental accuracy in all the range of temperatures and magnetic fields. This result casts doubt on the earlier assumption [2] that the reason for a strong magnetoelectric effect in the $HoAl_3(BO_3)$ crystal is the shift of atoms in the unit cell. In $Ho_{1-x}Y_xAl_3(BO_3)_4$ crystals

(x = 0.5, 1) there are no changes in the indirect hyperfine interaction parameters within the temperature range of 300-100 K. It was ascertained that in the $Ho_{1/2}Y_{1/2}Al_3(BO_3)$ mixed crystal the distribution of yttrium and holmium ions in the corresponding positions is close to equiprobable.

The authors acknowledge L. N. Bezmaternykh, I. A. Gudim, and V. L. Temerova for the provision of the samples and valuable discussions.

The work was supported by the Ministry of Education and Science of the Russian Federation, grant No. 8365.

REFERENCES

1. A. M. Kadomtseva, Yu. F. Popov, G. P. Vorob'ev, A. P. Pyatakov, S. S. Krotov, K. I. Kamilov, V. Yu. Ivanov, A. A. Mukhin, A. K. Zvezdin, A. M. Kuz'menko, L. N. Bezmaternykh, I. A. Gudim, and V. L. Temerov, *Low Temp. Phys*., **36**, 511 (2010).
2. K-C. Liang, R. P. Chaudhury, B. Lorenz, Y. Y. Sun, L. N. Bezmaternykh, I. A. Gudim, V. L. Temerov, and C. W. Chu, *J. Phys.: Conference Series*, **400**, 032046 (2012).
3. L. N. Bezmaternykh, V. L. Temerov, I. A. Gudim, and N. L. Stolbovaya, *Cryst. Rep*., **50**, Suppl. L, 97 (2005).
4. V. L. Temerov, A. E. Sokolov, A. E. Sukhachev,. A. F. Bovina, I. S. Edel'man, and A. V. Malakhovskii, *Cryst. Rep*., **53**, 1157 (2008).
5. E. L. Belokoneva, A. V. Azizov, Y. B. Leonjuk, M. A. Simonov, and N. B. Belov, *J. Struct. Chem.*, **22**, No. 3, 476-478 (1981).
6. A. Abragam, *The Principles of Nuclear Magnetism*, Clarendon Press, Oxford, UK (1961).
7. Koziro Narita, Jun-ichi Umeda and Hazime Kusumoto, *J. Chem. Phys*., **44**, 2719 (1966).
8. A. D. Mills, *Inorg. Chem*., **1**, 960 (1962).